J Geophys (1987) 62:50–61

Journal of Geophysics

Paleomagnetic investigation of Quaternary West Eifel volcanics (Germany): indication for increased volcanic activity during geomagnetic excursion/event?

H. Böhnel [1] *, N. Reismann [1] **, G. Jäger [1] *, U. Haverkamp [1] ****, J.F.W. Negendank [2], and H.-U. Schmincke [3]**

[1] Institut für Geophysik, Universität Münster, Corrensstraße 24, D-4400 Münster, Federal Republic of Germany
[2] Abteilung Geologie, Universität Trier, Postfach 3825, D-5500 Trier, Federal Republic of Germany
[3] Institut für Mineralogie, Ruhr-Universität Bochum, Postfach 102148, D-4630 Bochum, Federal Republic of Germany

Abstract. Eighty-five sites of West Eifel volcanoes were investigated paleomagnetically, giving 64 independent virtual geomagnetic poles (VGP). The VGP distribution is strongly asymmetric: about 30% of the VGPs have latitudes below 60° N and are confined to the longitude sector between 30° E and 120° E. This leads to a mean VGP situated at 74.0° N/63.9° E, deviating significantly from the north geographical pole. The VGP distribution is non-Fisherian, but the radial component is rather similar to that observed for Tertiary to Quaternary Icelandic lavas. Tectonic, petrographic, rock magnetic properties and secular variation do not seem to be responsible for the anomalous VGP positions. We propose that the volcanoes with anomalous VGPs erupted in a short period during an excursion or event of the earth's magnetic field.

Key words: Paleomagnetism – Virtual geomagnetic poles – Geomagnetic excursion/event – Volcanics – Ore petrography – Quaternary – West Eifel (Germany)

Introduction

Secular variation of the Quaternary magnetic field of East Eifel volcanics was studied by Kohnen and Westkämper (1978). The distribution of the VGPs obtained was largely Fisherian (Fisher, 1953), and their dispersion around the north geographic pole was in agreement with several models for the secular variation. Some lava flows were correlated to certain volcanic eruption centres based on paleomagnetic data (Böhnel et al., 1982). The results encouraged us to carry out similar studies in the nearby Quaternary volcanic field of the West Eifel. The main problems to be studied were: (1) to assign lava flows to one of the nearby eruption centres, (2) to obtain an approximate but independent control on radiometric age determinations of volcanics by polarity of magnetization and (3) to compare the secular variation of this region with that determined in the eastern part of the Eifel.

Present addresses:
* H. Böhnel, Instituto de Geofisica, Universidad Nacional Autonoma de Mexico, Del. Coyoacan, 04510 Mexico, D.F., Mexico
** N. Reismann, Mannesmann Kienzle, Waldstraße, D-7730 Villingen, Federal Republic of Germany
*** G. Jäger: BEB Erdgas und Erdöl GmbH, Riethorst 12, D-3000 Hannover, Federal Republic of Germany
**** U. Haverkamp: Radiologische Klinik, Roxeler Straße, D-4400 Münster, Federal Republic of Germany

Offprint requests to: H. Böhnel

The West Eifel volcanic field

The Quaternary West Eifel volcanic field (covering about 600 km^2) extends for 50 km NW-SE and comprises about 240 eruptive centres (Büchel and Mertes, 1982; Schmincke, 1982; Mertes, 1983; Schmincke et al., 1983) (Fig. 1). The basement consists of Devonian clastic sedimentary rocks and local Middle- to Upper-Devonian limestone, locally overlain by Triassic sandstones.

West Eifel volcanism started during the Pleistocene, the main activity about 0.7 M.a. ago, with the eruption of foiditic lavas, slightly post-dating the onset of the Pleistocene phase of uplift in the Rhenish massif (Illies et al., 1979; Lippolt and Fuhrmann, 1981; Mertes and Schmincke, 1983) and lasted to about 0.01 M.a. B.P. (Büchel and Lorenz, 1982). Rising magmas used dominantly NW-SE- and rarely N-S-oriented fractures as eruptive fissures (Mertes, 1983). The eruptive centres consist mainly of scoria cones (66%, about half of them with lava flows), 30% maars and tuff rings, about 2% scoria rings and 2% pyroclastic vents.

The Quaternary West Eifel lavas are dominantly leucitites and nephelinites (42% of the 174 eruptive centres studied), melilite-bearing foidites (32%), olivine-free foidites (ol < *1* vol.-%) (6%), olivine nephelinites (ol > *10* vol.-%) (5%), melilite-free sodalite-bearing foidites (4%), basanites (8%), tephrites (1%), phonolites (2%) (Mertes and Schmincke, 1985).

Mineralogically, the foidite suite is dominated by clinopyroxene (Ti-augite), accompanied by olivine and minor phlogopite phenocrysts. Phenocrystal olivine exceeds clinopyroxene in the younger (< 0.1 M.a.; Mertes and Schmincke, 1985) olivine-nephelinite and basanite suite which occurs mainly in the southeastern part of the field. Rare differentiated rocks – tephrites and phonolites – are restricted to the centre of the field and are characterized by leucite, sodalite, plagioclase and sanidine. A detailed petrographic description of West Eifel lavas is given by Mertes (1983).

About two-thirds of the volcanoes contain nodules, both of mantle-derived peridotites up to several decimetres in diameter and cumulates of low- to intermediate-pressure

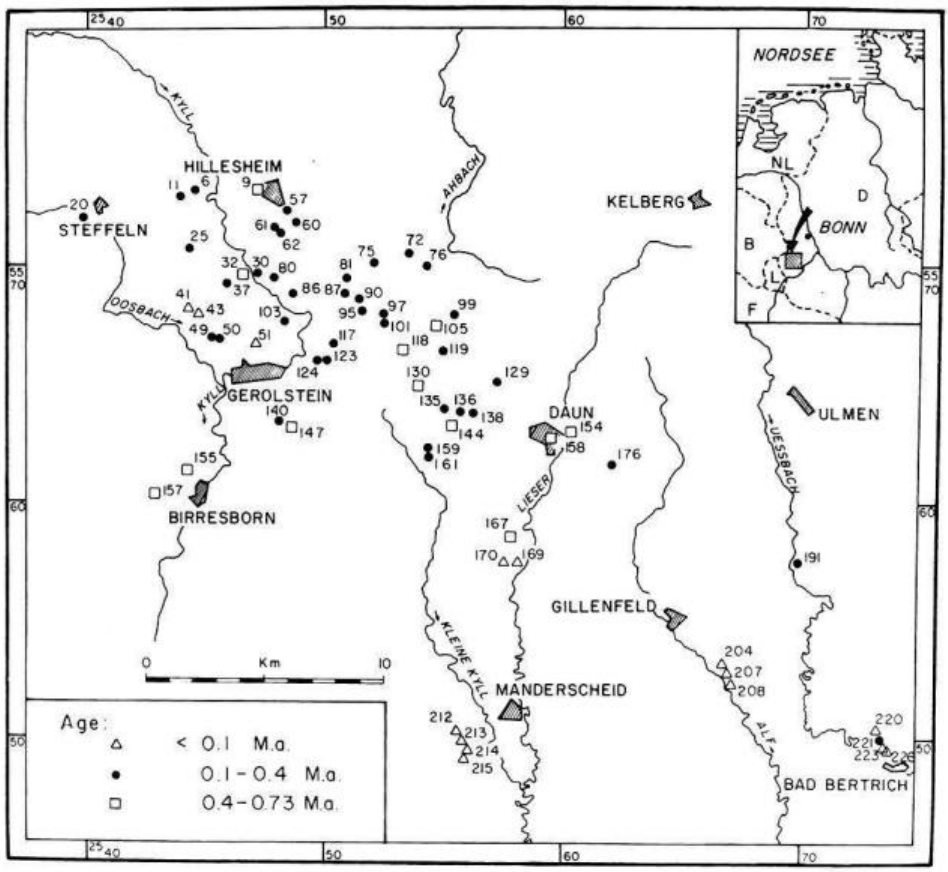

Fig. 1. Locations of sites sampled for paleomagnetic measurements. Three age ranges (according to Mertes and Schmincke, 1983) are indicated with different symbols. *Numbers* refer to Table 1 and to the eruption centre catalogue (Büchel and Mertes, 1982) for the West Eifel

Table 1. EC: eruption centre according to Büchel and Mertes (1982), different sites from one and the same eruption centre being distinguished by affixed letters and an uncertain correlation to this or a neighbouring eruption centre being indicated by the *symbol* #; topographic map and coordinates; name of site; chemical composition (*Bs*: basanite, *Lc*: leucitite, *Mel*: melilite nephelinite, *Ne*: nephelinite, *Ol*: olivine nephelinite; *Mel-b.Ne*: melilite-bearing nephelinite, *Ol-fr.Lc*: olivine-free leucitite, etc.); type of exposure (*plug*: volcanic plug, *tuff*: palagonite-tuff, *scor*: scoria, *sill*: sill-like flows within cinder cones); age estimates (geological evidence) and K/Ar ages ($^{40}Ar/^{39}Ar$ indicated by *star symbol*) for West Eifel volcanics sampled for paleomagnetic measurements according to Lippolt and Fuhrmann (1981) and Mertes and Schmincke (1983)

EC	Map	*r*-25	*h*-55	Name	Rock	Exp.	Age-Est.	Radiometric age
6a	5705	4470	7315	Ruderbüsch I	Lc-Ne	flow	0.1–0.4	
6b	5705	4495	7315	Ruderbüsch II	Lc-Ne	dike	0.1–0.4	
9	5705	4715	7305	Steinrausch	Ne-Lc	scor	0.4–0.73	1.37 ± 0.04
11	5705	4410	7260	Basberg	Lc-Ne	flow	0.4–0.73	
14	5705	5270	6900	Mühlenberg	Mel-Ne	flow		
20	5705	3920	7205	Steffelner Kopf	Lc-Ne	flow	0.1–0.4	
25	5705	4490	7135	Rossbüsch	Mel-Ne	flow	0.1–0.4	
30	5705	4715	6965	Dohm	Lc-Ne	flow	0.1–0.4	
32	5705	4655	6900	Beilstein	Lc-Ne	flow	0.1–0.4	
37	5705	4580	6925	Wolfsbeuel	Lc-Ne	dike	0.1–0.4	
41	5705	4420	6820	Rother Kopf II	Mel-b.Ne	flow	0.1–0.4	
43	5705	4440	6800	Rother Kopf I	Mel-b.Ne	sill	0.1–0.4	
49	5705	4500	6650	Rother Hecke I	Mel-Ne	flow	0.1–0.4	
50	5705	4545	6695	Rother Hecke II	Ne-Lc	dike	0.1–0.4	
51	5705	4670	6540	Sarresdorf	Bs	flow	0.1–0.4	
57	5706	4800	7210	Am Lier	Mel-Ne	flow	0.1–0.4	
60	5706	4910	7180	Kyller Höhe	Mel-Ne	flow	0.1–0.4	
61	5706	4775	7195	Graulei I	Lc?	flow	0.1–0.4	
62	5706	4820	7080	Graulei III	Mel-Ne	flow	0.1–0.4	
72a	5706	5345	7075	Kahlenberg Süd	Ne-Lc	flow	0.1–0.4	
72b	5706	5385	7065	Kahlenberg	Ne-Lc	dike	0.1–0.4	
75	5706	5190	6995	Gonnenstall	Ne	flow	0.1–0.4	
76	5706	5440	6995	Döhmberg	Lc	scor	0.1–0.4	
80a	5706	4750	6925	Giesenheld I	Lc-Ne	flow	0.1–0.4	
80b	5706	4755	6960	Giesenheld II	Lc-Ne	flow	0.1–0.4	

Table 1 (continued)

EC	Map	*r*-25	*h*-55	Name	Rock	Exp.	Age-Est.	Radiometric age
81	5706	5085	6980	Am Köpfchen	Lc-Ne	flow	0.1–0.4	
86	5706	4840	6840	Rockeskyller Kopf	Lc-Ne	flow	0.1–0.4	0.63 ± 0.03, 0.36 ± 0.04, 0.44 ± 0.04
87	5706	5080	6870	Gyppenberg	Mel-Ne	sill	0.1–0.4	
90	5706	5140	6850	Bickenberg	Mel-b.Ne	dike	0.1–0.4	
94	5706	5215	6810	Feuerberg	Mel-b.Ne	plug	0.1–0.4	
95a	5706	5150	6800	Alter Voß I	Ne-Lc	scor	0.1–0.4	
95b	5706	5150	6800	Alter Voß II	n.d.	dike	0.1–0.4	
95c	5706	5100	6750	Alter Voß III	Ne-Lc	flow	0.1–0.4	
97a	5706	5260	6820	Feuerberg	Mel-b.Ne	dike	0.1–0.4	
97b	5706	5250	6760	Feuerberg	Mel-b.Ne	flow	0.1–0.4	
97c	5706	5190	6750	Feuerberg	Mel-b.Ne	flow	0.1–0.4	
99	5706	5540	6845	Dockweiler	Ne-Lc	flow	0.1–0.4	
99	5706	5625	6945	Steinlei	n.d.	flow	0.1–0.4	
101	5706	5230	6760	Auf Winkel	Ne	flow	0.1–0.4	
105	5706	5450	6750	Hangelberg	Lc	dike	0.1–0.4	
103#	5706	4800	6770	Hahn	Mel-Ne	flow	0.1–0.4	
117	5706	5020	6640	Sellbüsch	Mel-b.Ne	flow	0.1–0.4	
118	5706	5335	6650	Beuel/Kirchweiler	Mel-b.Ne	plug	0.4–0.73	2.09 ± 0.10
119	5706	5520	6620	Ernstberg	Ol-fr.Ne-Lc	flow	0.1–0.4	
123a#	5706	4980	6600	Baarley II	Ol-fr.Lc	dike	0.1–0.4	
123b#	5706	4980	6600	Baarley I	Ol-fr.Lc	sill	0.1–0.4	
129	5706	5705	6540	Asseberg	Ne	flow	0.1–0.4	
130	5706	5385	6490	Scharteberg	Ol-fr.Hau-Ne	scor	0.4–0.73	0.51 ± 0.2
135	5706	5505	6395	Goosberg	Mel-b.Ne	scor	0.1–0.4	
136	5706	5505	6450	Hippersbach		tuff	0.1–0.4	
138	5706	5595	6380	Held		tuff	0.1–0.4	
140	5706	4785	6335	Krekelsberg	Mel-b.Ne	flow	0.1–0.4	
144	5706	5535	6320	Riemerich	Mel-b.Ne	flow	0.4–0.73	2.34 ± 0.05
147	5706	4840	6320	Dietzenley	Mel-b.Ne	plug	0.4–0.73	2.73 ± 0.15, 0.62 ± 0.11, 0.62 ± 0.15*
154	5707	5990	6300	Firmerich	Ne-Lc	flow	0.4–0.73	0.75 ± 0.04, 0.95 ± 0.18, 0.60 ± 0.14*
155a	5705	4510	6205	Kalem	Mel-Ne	flow	0.4–0.73	0.82 ± 0.03,
155b	5705	4510	6205	Kalem	Mel-Ne	flow	0.4–0.73	0.66 ± 0.16, 0.54 ± 0.18*
157a	5805	4280	6040	Fischbachtal West	Lc-Ne	flow	0.4–0.73	
157b	5805	4360	6025	Fischbachtal Ost	Ne	flow	0.4–0.73	
158	5806	5885	6290	Burgberg	Mel-b.Ne	plug	0.4–0.73	
159	5806	5435	6230	Nerother Kopf	Lc-Ne	flow	0.1–0.4	
161	5806	5432	6200	Kahlenberg/Neroth	Lc-Ne	dike	0.1–0.4	
167	5806	5815	5815	Üdersdorf (Liley)	Mel-Ne	flow	0.4–0.73	0.74 ± 0.09
169	5806	5800	5750	Mühlenkaul I	Ol-Ne	flow	<0.1	
170a	5806	5740	5740	Emmelberg	Ol-Ne	sill	<0.1	
170b	5806	5785	5735	Emmelberg II	Ol-Ne	scor	<0.1	
176	5807	6200	6150	Auf der Haardt	Ne-Lc	scor	0.1–0.4	
191	5807	6980	5730	Roter Berg	Ne-Lc	scor	0.1–0.4	
204	5807	6685	5320	Wartgesberg Nord	Bs	scor	<0.1	
207a	5807	6680	5285	Wartgesberg	Bs	scor	<0.1	0.23 ± 0.10
207b	5807	6675	5285	Wartgesberg Ost	Bs	dike	<0.1	0.23 ± 0.10
208a#	5807	6655	5285	Strohner Mühlen	Bs	scor	<0.1	
208b#	5807	6680	5265	Strohner Mühlen	Bs	scor	<0.1	
208c#	5807	6670	5235	Alftal	Bs	flow	<0.1	
212	5906	5555	5040	Windsborn	Ol-Ne	scor	<0.1	
213#	5906	5555	4970	Mosenberg	Ol-Ne	dike	<0.1	
215a#	5906	5585	4985	Mosenberg	Ol-Ne	scor	<0.1	
215b#	5906	5560	4960	Mosenberg	Ol-Ne	sill	<0.1	
215c#	5906	5580	4925	Mosenberg	Ol-Ne	sill	<0.1	
215d#	5906	5740	4905	Horngraben	Ol-Ne	flow	<0.1	
220	5908	7285	4985	Falkenley	Bs	flow	<0.1	
221a	5908	7320	4915	Bad Bertrich	Bs	flow	<0.1	1.16 ± 0.04,
221b	5908	7280	4950	Bad Bertrich	Bs	flow	<0.1	0.06 ± 0.03
223	5908	7360	4950	Dachslöcher	Bs	flow	<0.1	
224	5908	7330	4960	Facher Höhe	Bs	flow	<0.1	

origin (Sachtleben and Seck, 1981; Stosch and Seck, 1980; Mertes, 1983; Duda and Schmincke, 1985).

Sampling

Eighty-five sites were sampled, based on the detailed fieldwork of Büchel and Mertes (1982) and in coordination with H. Mertes. These sites represent 73, and thus one-third, of all known eruption centres in the West Eifel. Further paleomagnetic sampling is not possible because suitable exposures of the remaining maars and cinder cones are lacking.

Table 1 lists the sites with their coordinates, rock type, type of exposures and estimated ages (geological evidence) or radiometric ages. Most sites are in lava flows, others are from dikes and sill-like small flows within scoria cones, plugs and two palagonite tuffs.

To avoid systematic errors due to local tectonic movements, 8–12 cores distributed over an entire site were taken with a portable gasoline-powered corer. The cores were oriented with an inclinometer and a magnetic and/or a sun compass (Collinson, 1983).

Laboratory procedures

The cores were subdivided into 21-mm-long specimens. Generally, the specimens were demagnetized with alternating-field static or tumbling demagnetizers. Only a few selected samples were thermally demagnetized. Intensity and direction of magnetization were determined with a Digico-Spinner magnetometer (Molyneaux, 1971), magnetic susceptibility with a Bison bridge 3101 A and in part with a Minisep bridge (Molspin Ltd.), which was also used for measurements of anisotropy of magnetic susceptibility (AMS). IRM-acquisition curves and reversed-field demagnetization curves were obtained using a pulse magnetizer producing up to 1200 kA/m. H_c and M_s were determined with a hysteresis curve tracer similar to the instrument described by Likhite et al. (1963), in fields up to 160 kA/m. Polished sections were studied in reflected light and scanning electron microscope (SEM) (Cambridge S 250 Mk II with Link semiquantitative microanalyser for the determination of elements with atomic weight >20).

For each site, three or more pilot specimens were demagnetized in at least seven steps, depending on the directional behaviour of magnetization. The characteristic remanent magnetization (CARM) was then determined using Zijderveld diagrams (Zijderveld, 1967), stability indices (Symons and Stupavsky, 1974) and analysis of demagnetization paths (Kirshvink, 1980) and difference-vector variations (Hoffman and Day, 1978). Whenever all pilot specimens from one site exhibited simple and similar variations of magnetization direction, the remaining specimens were all demagnetized in 3–5 selected steps of coinciding field strengths. Otherwise, every specimen was demagnetized individually in seven or more steps.

Experimental results

Only results from standard treatment of specimens from all sites, i.e. demagnetization and ore petrography, are regarded. Further measurements made on selected specimens are discussed later.

Ore petrography

One or more polished sections were prepared for most sites and studied by reflected light microscopy and SEM. Table 2 contains results separated for the most common oxides and minor important oxides. Most oxides are titanomagnetites in the range 3 μm (pigment) to about 60 μm, phenocrysts often exceeding 100 μm. Anhedral grains dominate, but euhedral grains were also observed, most of which are smaller than 10 μm.

Titanomagnetites (TM) commonly contain impurities ($<3\%$) of Al, Mn, Mg and Cr. The TiO_2 content ranges between 3% and about 26%. Most TM belong either to the oxidation class 1 or 5 and 6 (Ade-Hall et al., 1968; Wilson and Haggerty, 1966). The less oxidized grains are largely maghemitized and/or granulated, presumably resulting from hydrothermal alteration.

Subordinate TM were observed belonging to another oxidation class, e.g. they are less oxidized or more oxidized than the dominating ore phase. Some samples contained chromite, ilmenite, ilmenite-hematite, hematite, ferritespinels and pyrite. In 11 samples, secondary hematite formed from olivine and augite.

Figure 2 shows typical examples of SEM: TM of HT-oxidation class *1*, partly euhedral, with grain diameters of about 20 μm are typical for many rocks (Fig. 2a). Many TM suffered maghemitization at a different degree. Figure 2b shows the typical maghemitization shrinking cracks (Wilson and Haggerty, 1966). An example for strongly oxidized TM is given in Fig. 2c. The grains are dissolved, partly persisting only as a hematite skeleton. Some hematite skeletons resulted from alteration of olivine (Fig. 2d).

Magnetic properties

Table 3 (columns 2–6) lists site mean values for the NRM intensity M_0, the intensity M_8 after af demagnetization with 8 kA/m, susceptibility χ, Königsberger factor Q and the medium destructive field MDF. One representative sample per site was subjected to magnetic hysteresis measurements at field strengths up to 160 kA/m. Saturation magnetization M_s, coercive force H_c and the corresponding values of the remanent hysteresis curve, M_{rs} and H_{cr}, are given in the last four columns.

All magnetic properties range widely. NRM intensity ranges between 0.6 and 60 A/m and susceptibility between 0.003 and 0.1 m^3/m^3 (Fig. 3). In correspondence with petrographic observations, low values are due to strong high-temperature oxidation and/or hydrothermal alteration, with partial transformation of strongly magnetic TM to weakly or non-magnetic oxidation products. The Q factor generally has values greater than about *1*, indicating the presence of (pseudo-) single-domain particles (Day, 1977).

There is no obvious correlation of magnetic parameters with rock composition. Only melilite-nephelinites have higher susceptibilities at quite normal NRM intensities, which results in comparatively small Q factors between *1* and 3. The high-temperature oxidation number M_{ox} is generally *1* for these rocks, whereas the other rock types are more oxidized ($M_{ox}=4 \ldots 6$) and have higher Q factors between 3 and 30. This is most likely due to the reduction of grain size by exsolution lamellae. This interpretation is further supported by the fact that rocks with high M_{ox} values also exhibit high MDF values.

Scoria shows greater magnetic stability than lava, be-

Table 2. Petrographic results from reflected light microscopy and SEM. Left part represents dominating titanomagnetites, right subordinate oxides. EC: eruption centre; grain diameter *d*; grain form: *eu*: euhedral, *sub*: subhedral, *an*: anhedral; high-temperature oxidation number M_{ox}; TiO_2 content and contamination of titanomagnetite by Al, Mn, Mg, Cr; granulation, dissolution and maghemitization of grains; *TM*: titanomagnetites with low-temperature oxidation number M_{ox}; other oxides: *Cr*: chromite, *Hem*: hematite, *Mag*: magnetite, *Il*: ilmenite, *Sec. Hem*: secondary hematite

	Dominant ore phase											Subordinate ore phases		
EC	*d* (μm)	Grain form	M_{ox}	TiO_2 wt.-%	Al	Mn	Mg	Cr	Gran	Diss	Magh	TM M_{ox}	Other	Sec. Hem
6	<40	sub	1	20		×					×	–	Cr	
25	5– 50	eu-an	1	19		×					×	–		
57	5– 50	eu-an	1	18–19		×	×				×	–	Cr	
72b	4– 60	eu-an	3–5	22	×	×	×		×			1–2		
72a	2– 30	an	5	11					×	×		1–2		
86	6– 60	eu-an	3–4									5	Cr	
94	4– 60	eu-an	6	10–12		×	×			×		–	Ferrit	
97a	2– 30	an	6							×		–	Hem, Ferrit	×
97b	4– 40	eu-an	6	16			×	×				1		
99	2– 60	eu-an	3–5						×			1–2	Pyrit	
117	4– 30	eu-an	1	20		×					×	–		
118	5– 50	eu-an	1	19							×	–		
119	4– 60	an	1–2	16		×					×	–		
129	<30	eu-sub	1	20		×					×	–		
130	2– 80	an	6	10						×		1		×
135	10–100	an	6									3	Mag	
140	10– 20	eu-an	1	18		×	×				×	–		
144	5–100	an	6	16								3–4	Mag	
147	5– 50	eu-an	1	22		×					×	–	Hem	
154	2– 40	eu-an	1	18		×					×	1–2		
155a	6– 60	eu-sub	1	17	×		×					–		
155b	3– 60	eu-an	1	19–24		×					×	–		
157	4– 30	eu-an	6	4						×		4–5		×
158	10– 20	eu-an	1	18–21	×	×	×	×			×	–		
204	< 4	eu-an	6	23								–	Cr, Il	×
207a	<10	an	1	22			×				×	–		×
207b	< 5	eu-an	3		×							–	Cr	×
208b	10	eu-an	6									–	Hem	
208c	4– 40	eu-an	1	26				×			×	–		
212	4– 20	eu-an	1	16			×					1–2		
213	5– 60	eu-an	4–6	26					×	×		3	Cr, Il-Hem	×
215a	<50	eu-an	Chromite									1		×
215b	3– 80	eu-an	3–6	4					×	×		1–2	Cr, Hem	
215b	3– 50	eu-an	1		×		×				×	–	Il-Hem	
215c	4– 40	an	6							×		5	Cr	
221	<10	eu	1	26			×		×			1–2	Cr	
223	<30	an	5									3–4	Cr, Mag	

cause faster cooling resulted in smaller TM grain sizes and, therefore, more (pseudo-) single-domain particles.

Hysteresis values of selected samples (Table 3) are subjected to a domain-structure diagnosis (Day et al., 1977; Dunlop, 1981). Figure 4 suggests the occurrence of predominantly pseudo-single-domain particles which are believed to have high stability of remanence.

Paleodirections and VGP distribution

Table 4 lists the paleomagnetic results. If different sites were suspected of belonging to the same eruption centre, their data were subjected to the F-test. The lower part of Table 4 lists those sites from one and the same eruption centre or from several coeval eruption centres within one volcanic complex, together with their mean direction and statistical parameters.

Figure 5a shows the remaining 64 independent directions and VGPs in equal-area plots. Error circles α_{95} are not given, as this would totally obscure the distribution of directions and poles. The directions/VGPs are of normal polarity. These rocks studied probably erupted during the Brunhes epoch and are thus younger than 0.73 M.a. These data have been one of the constraints in postulating that apparent K/Ar ages older than 0.73 M.a. are probably in error due to excess argon (Mertes and Schmincke, 1983).

Many directions clearly diverge from the dipolar direction of the earth's magnetic field. This also holds for the mean direction. The VGP distribution is strongly asymmetric: a considerable part has latitudes $<60°$ and is concentrated in the longitude sector between 30° E and 120° E. Consequently, the mean VGP lies at 63.9° E/74.0° N and the error circle α_{95} indicates a significant departure from the north geographical pole (NGP).

The VGP density distribution (Fig. 5b) shows two clearly separated maxima: one near the NGP with the cor-

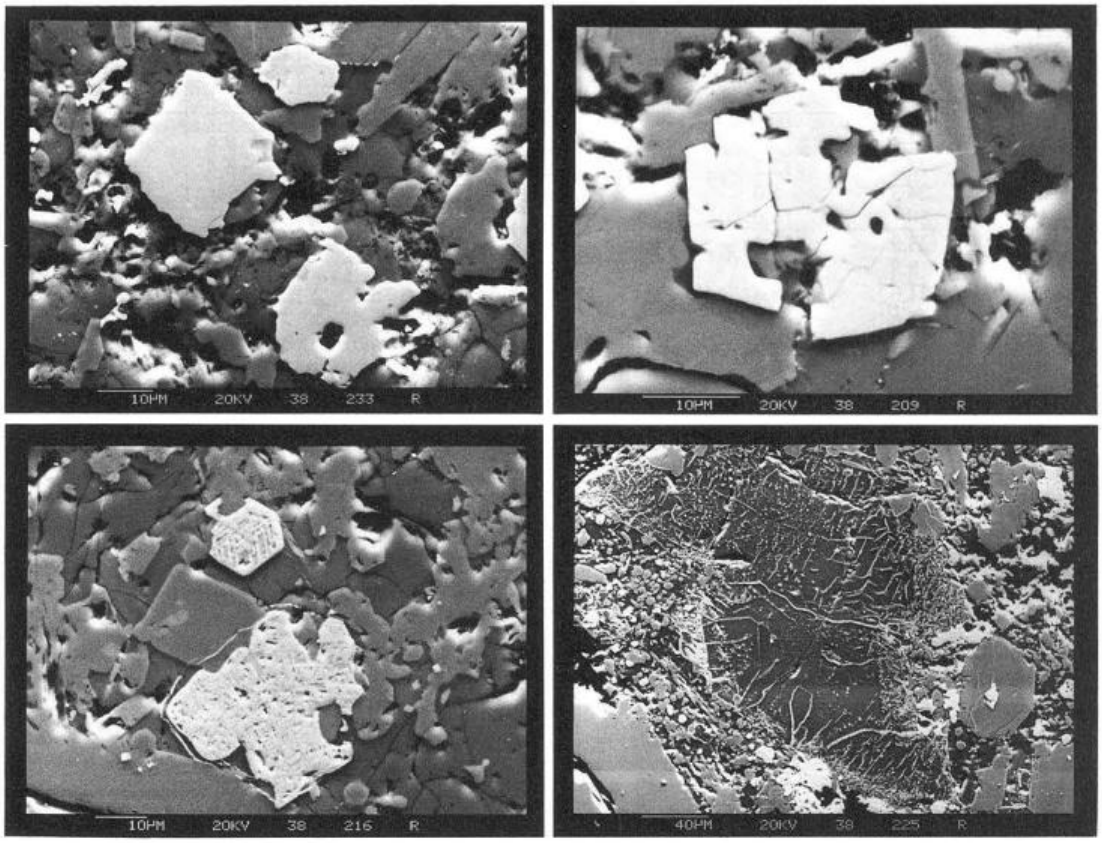

Fig. 2a–d. Examples for SEM studies on polished sections. **a** partly anhedral titanomagnetites, typical for many specimens; **b** maghemitized titanomagnetite; **c** strongly oxidized titanomagnetite; **d** hematite skeleton as alteration product of olivine

Table 3. Rock magnetic properties. Eruption centre; mean NRM intensity M_0, mean intensity M_8 after af demagnetization with 8 kA/m; susceptibility χ and Q factor; medium destructive field MDF; saturation magnetization M_s; remanent saturation magnetization M_{rs}; coercive force H_c; remanent coercive force H_{cr}; n.d. not determined

EC	M_0 (A/m)	M_8 (A/m)	χ (10^{-3})	Q	MDF (kA/m)	M_s (kA/m)	M_{rs} (kA/m)	H_c (kA/m)	H_{cr} (kA/m)
6a	2.9	1.6	32.0	3.0	15	n.d.	n.d.	n.d.	n.d.
6b	4.6	2.4	35.3	3.4	10	n.d.	n.d.	n.d.	n.d.
9	2.4	2.9	46.1	2.4	10	n.d.	n.d.	n.d.	n.d.
11	2.9	1.7	91.3	0.8	10	9.0	0.5	4.0	14.4
14	2.7	n.d.	44.1	3.4	12	n.d.	n.d.	n.d.	n.d.
20	9.2	5.5	20.7	11.6	16	0.55	0.55	10.4	16.9
25	4.3	1.8	51.6	2.2	13	n.d.	n.d.	n.d.	n.d.
30	4.0	2.5	46.3	2.2	10	3.9	0.66	6.4	14.4
32	8.7	5.3	51.3	4.4	8	5.0	1.34	10.8	23.4
37	4.2	3.8	25.2	4.3	31	0.35	0.08	12.4	15.2
41	4.8	2.2	18.1	6.9	11	3.8	1.13	12.8	37.8
43	11.7	2.8	33.3	9.2	13	1.35	0.20	3.2	9.6
49	19.8	n.d.	71.1	7.3	4	n.d.	n.d.	n.d.	n.d.
50	3.5	1.9	23.4	3.9	9	2.6	0.69	9.6	16.8
51	5.1	3.9	18.1	7.3	12	n.d.	n.d.	n.d.	n.d.
57	2.7	0.6	57.4	1.2	n.d.	n.d.	n.d.	n.d.	n.d.
60	1.3	0.5	67.0	0.5	15	3.99	1.09	12.8	40.0
61	1.0	0.6	54.8	0.4	11	8.25	0.38	5.6	24.0
62	1.4	0.4	116.8	0.3	5	7.25	1.04	5.6	21.8
72a	4.1	2.1	50.3	2.2	12	n.d.	n.d.	n.d.	n.d.
72b	16.9	1.5	14.0	31.4	15	n.d.	n.d.	n.d.	n.d.
75	5.9	2.4	87.6	1.7	10	9.0	1.50	9.6	27.2
76	3.5	4.4	2.8	32.5	70	n.d.	n.d.	n.d.	n.d.
80a	7.6	2.7	13.8	14.4	25	1.9	0.49	10.4	29.0
80b	58.6	17.8	80.9	19.0	6	4.75	0.70	6.4	13.8
81	4.6	2.6	43.1	2.8	19	4.1	0.72	16.3	27.3
86	2.4	0.9	39.8	1.8	21	n.d.	n.d.	n.d.	n.d.

Table 3 (continued)

EC	M_0 (A/m)	M_8 (A/m)	χ (10^{-3})	Q	MDF (kA/m)	M_s (kA/m)	M_{rs} (kA/m)	H_c (kA/m)	H_{cr} (kA/m)
87	7.7	4.8	43.1	2.8	19	4.4	1.10	9.6	37.6
90	34.9	12.2	75.2	12.2	4	8.5	1.21	6.4	19.2
94	3.2	1.2	24.3	5.0	60	n.d.	n.d.	n.d.	n.d.
95a	42.7	5.1	80.1	14.0	2	1.4	0.15	3.2	12.8
95b	30.3	25.2	23.9	33.3	16	0.51	0.12	8.1	32.4
95c	3.8	2.3	8.8	11.3	25	0.85	0.32	23.6	32.4
97a	4.6	2.0	21.0	8.4	24	n.d.	n.d.	n.d.	n.d.
97b	9.0	5.5	45.8	5.4	4	n.d.	n.d.	n.d.	n.d.
97c	1.9	0.9	7.1	7.7	37	n.d.	n.d.	n.d.	n.d.
99a	1.8	n.d.	38.3	8.0	6	n.d.	n.d.	n.d.	n.d.
99b	3.4	3.0	38.9	2.3	30	5.0	0.61	4.0	13.8
101	6.4	3.4	36.2	5.4	7	n.d.	n.d.	n.d.	n.d.
103#	16.6	6.7	25.3	17.2	8	1.2	0.71	10.4	25.6
105	10.0	3.5	6.7	39.2	53	0.95	0.21	66.1	117.3
117	15.3	n.d.	75.0	5.3	2	n.d.	n.d.	n.d.	n.d.
118	17.8	2.5	97.1	4.8	5	n.d.	n.d.	n.d.	n.d.
119	10.0	3.2	31.2	8.3	6	n.d.	n.d.	n.d.	n.d.
123a#	7.9	0.6	68.0	3.0	5	10.0	1.78	9.6	25.6
123b#	0.7	2.5	7.4	2.4	29	0.3	0.12	48.0	57.2
129	2.4	0.7	61.4	1.2	9	n.d.	n.d.	n.d.	n.d.
130	6.3	1.8	11.9	13.8	10	n.d.	n.d.	n.d.	n.d.
135	3.7	n.d.	8.1	12.1	4	n.d.	n.d.	n.d.	n.d.
136	0.5	0.2	12.2	1.2	5	n.d.	n.d.	n.d.	n.d.
138	0.4	0.2	8.9	1.2	12	n.d.	n.d.	n.d.	n.d.
140	3.8	1.7	53.9	1.8	9	n.d.	n.d.	n.d.	n.d.
144	3.4	1.2	3.1	30.6	24	n.d.	n.d.	n.d.	n.d.
147	32.0	2.6	36.5	22.8	6	n.d.	n.d.	n.d.	n.d.
154	4.0	2.9	33.3	3.1	22	n.d.	n.d.	n.d.	n.d.
155a	4.4	2.7	71.7	2.5	8	n.d.	n.d.	n.d.	n.d.
155b	3.9	n.d.	58.6	2.6		n.d.	n.d.	n.d.	n.d.
157a	1.9	n.d.	12.0	4.1	20	n.d.	n.d.	n.d.	n.d.
157b	3.6	1.7	61.1	2.7	20	n.d.	n.d.	n.d.	n.d.
158	4.0	0.7	70.7	1.5	2	n.d.	n.d.	n.d.	n.d.
159	4.3	3.8	19.8	8.6	22	n.d.	n.d.	n.d.	n.d.
161	4.3	3.5	42.2	2.6	22	7.12	2.0	14.4	33.3
167	3.7	2.2	88.5	1.2	11	n.d.	n.d.	n.d.	n.d.
169	89.1	6.2	8.8	19.7	32	0.52	0.21	12.1	22.3
170a	4.1	3.4	7.2	14.9	24	0.4	0.14	9.6	24.8
170b	7.3	5.9	5.8	33.1	42	0.4	0.06	54.4	79.5
176	1.1	1.0	3.8	7.6	44	0.4	0.06	52.8	60.0
191	5.7	4.6	5.2	28.8	38	0.9	0.16	67.2	78.5
204	7.8	2.9	10.0	20.7	39	n.d.	n.d.	n.d.	n.d.
207a	11.2	7.9	11.2	26.0	63	n.d.	n.d.	n.d.	n.d.
207b	8.9	13.1	15.0	15.4	27	n.d.	n.d.	n.d.	n.d.
208a#	7.8	9.8	8.1	25.1	29	n.d.	n.d.	n.d.	n.d.
208b#	12.8	9.9	21.5	15.5	25	n.d.	n.d.	n.d.	n.d.
208c#	4.3	2.5	29.4	3.8	14	n.d.	n.d.	n.d.	n.d.
212	14.9	10.6	11.9	32.5	46	n.d.	n.d.	n.d.	n.d.
213#	7.7	2.8	9.8	20.5	15	n.d.	n.d.	n.d.	n.d.
215a#	13.4	n.d.	10.5	33.2	15	n.d.	n.d.	n.d.	n.d.
215b#	26.0	n.d.	33.1	20.5	20	n.d.	n.d.	n.d.	n.d.
215c#	8.8	3.5	8.8	26.0	28	n.d.	n.d.	n.d.	n.d.
220	3.8	2.7	20.8	5.1	29	n.d.	n.d.	n.d.	n.d.
221a	6.6	4.6	22.1	7.9	9	n.d.	n.d.	n.d.	n.d.
221b	10.4	2.8	18.2	14.0	8	n.d.	n.d.	n.d.	n.d.
223	4.8	4.3	18.7	7.9	24	n.d.	n.d.	n.d.	n.d.
224	7.5	3.2	23.2	13.5	19	n.d.	n.d.	n.d.	n.d.

responding VGP distribution resembling that of other Quaternary distributions, e.g. from the East Eifel (Kohnen and Westkämper, 1978). The other maximum at about 60° N/45° E leads to the mean pole diverging from the NGP. This is in strong contrast to results from the East Eifel. Here the mean VGP coincided with the NGP and the distribution of the VGPs followed a Fisherian distribution.

The observed azimuthal and radial distributions around the mean VGP and the NGP, respectively, are compared with the corresponding theoretical curves according to Fish-

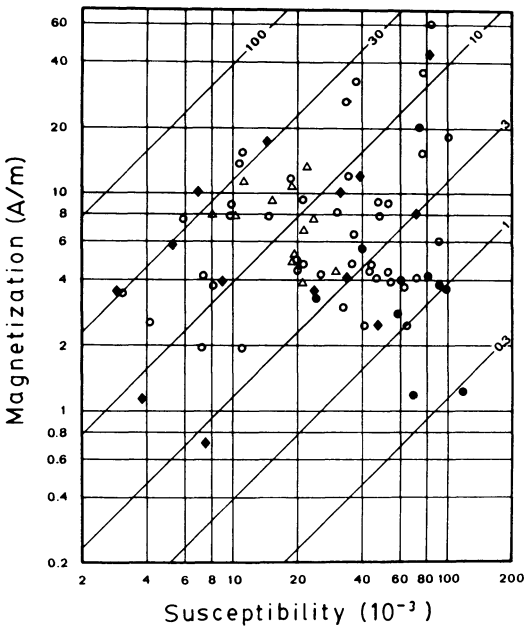

Fig. 3. Site mean values for NRM intensity (in A/m) plotted against site mean susceptibility. *Diagonals* indicate lines of constant Q factor. Chemical composition of rocks is given by different symbols. *Circles:* Melitite-nephelinites; *open circles:* nephelinites; *rhomboids*: leucitites; *open triangles:* basanites

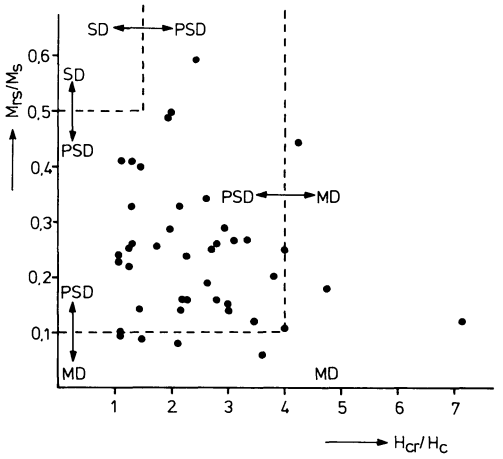

Fig. 4. H_{cr}/H_c plotted against M_{rs}/M_s for selected samples. Different domain configurations for magnetite (Dunlop, 1981) are marked: SD = single-domain, PSD = pseudo-single-domain, MD = multi-domain

er (1953) (Fig. 6). Radial and/or azimuthal observed and theoretical curves clearly diverge. Mathematically, this can be demonstrated using the χ^2-test (Table 5). The radial or azimuthal, or both theoretical and observed distributions, diverge significantly. The VGPs do not, therefore, follow a Fisherian distribution.

Kristjansson and McDougall (1982), in the most comprehensive compilation of data from Tertiary and Quaternary Icelandic volcanics, also observed a higher than expected percentage of low-latitude VGPs. They combined a Fisherian distribution with $k = 8.5$ and a 10% portion of statistically distributed VGPs as a satisfactory approximation of the observed VGP distribution. According to Fig. 6, this radial distribution (dashed line) fits the data

Table 4. Paleomagnetic results. Eruption centre; number n_s/n of samples studied/used for site mean calculation; precision parameters k and α_{95}; site mean declination/inclination Dec/Inc; VGP latitude/longitude Lat/Long. The lower part of the table comprises mean values calculated for two or more sites

EC	n_s/n	k	α_{95} (°)	Dec (°E)	Inc (°)	Lat (°N)	Long (°E)
6a	9/ 7	1126	1.7	65.2	73.2	52.8	57.6
6b	11/11	63	5.8	60.5	73.6	55.3	57.3
9	10/ 9	170	3.9	58.5	75.9	56.7	51.0
11	14/14	249	2.5	102.7	73.8	36.4	44.2
14	22/17	273	2.2	24.4	57.0	68.6	123.1
20	11/10	196	3.5	47.1	75.3	62.0	53.2
25	12/12	49	6.2	13.6	78.8	70.6	21.7
30	13/11	67	5.6	347.8	64.5	80.9	255.9
32	10/10	72	5.8	19.2	66.6	77.5	95.9
37	8/ 7	112	5.7	8.7	66.6	84.3	104.8
41	13/13	500	1.9	94.3	70.7	37.1	52.4
43	15/14	148	3.3	88.9	71.7	40.4	53.0
49	11/10	13	14.1	350.9	24.6	51.9	201.1
50	8/ 7	72	7.1	16.7	61.7	76.4	122.9
51	11/ 9	200	3.6	5.0	66.1	86.3	122.9
57	12/12	No stable remanence was determined					
60	13/ 6	84	7.4	101.7	80.2	43.2	33.7
61	12/12	133	3.8	57.6	73.3	56.7	59.0
62	13/13	78	4.7	55.7	75.9	58.1	51.3
72a	11/10	77	5.5	96.4	68.0	33.6	55.2
72b	11/ 9	133	4.4	96.8	78.0	42.7	38.6
75	13/11	103	4.5	21.5	66.5	76.1	93.8
76	11/10	758	1.7	90.1	76.7	43.6	43.1
80a	11/ 9	61	6.6	347.6	58.7	76.0	230.2
80b	11/ 7	51	8.5	354.4	58.1	77.8	207.8
81	13/13	204	2.9	49.6	77.6	60.6	45.3
86	10/ 9	310	2.9	35.7	54.1	59.8	114.0
87	12/12	203	3.1	72.1	77.5	51.5	45.0
90	8/ 6	48	9.8	337.3	67.6	75.5	286.2
94	9/ 9	473	2.3	51.6	72.0	59.4	63.7
95a	5/ 5	470	3.5	350.8	86.7	56.8	4.8
95b	6/ 5	No stable remanence was determined					
95c	8/ 8	256	3.4	42.5	46.3	64.3	56.5
97a	10/10	367	2.5	58.2	78.8	56.9	41.7
97b	10/ 9	39	8.3	33.0	63.7	67.4	96.3
97c	9/ 9	167	3.9	9.3	75.1	77.1	26.6
99a	15/ 8	76	6.3	45.1	65.2	60.5	84.7
99b	14/12	102	4.3	18.0	65.3	77.8	103.2
101	10/10	94	4.3	26.0	76.0	70.7	43.1
103#	14/11	128	4.1	24.5	62.8	72.4	107.4
105	16/13	23	8.8	358.1	64.2	85.5	203.8
117	11/10	35	8.2	79.8	31.0	19.5	93.8
118	12/12	71	5.1	352.0	88.3	53.5	5.9
119	12/ 8	28	10.5	24.4	53.5	65.9	129.4
123a#	12/ 8	23	11.7	38.9	42.4	50.6	122.7
123b#	11/11	78	5.2	58.4	33.8	34.2	109.2
129	8/ 8	93	5.7	322.4	56.0	59.8	264.4
130	10/ 9	222	3.4	244.3	77.4	36.1	339.7
135	11/11	127	4.0	13.2	63.2	79.5	123.3
136	12/11	47	6.7	21.7	74.9	73.4	44.8
138	11/10	52	6.7	12.3	67.2	82.1	93.9
140	11/10	149	3.9	9.6	71.9	81.2	43.7
144	11/10	173	3.6	38.1	57.2	60.3	106.7
147	13/ 7	63	7.6	6.8	64.4	84.0	134.5
154	13/12	229	2.8	64.4	72.3	53.0	57.4
155a	32/29	60	3.4	15.9	69.2	79.8	76.0
155b	10	45	7.1	21.7	62.0	73.6	113.4
157a	8/ 8	97	5.6	53.9	54.4	48.4	96.9
157b	9/ 7	96	6.1	60.3	49.7	41.5	96.8
158	10/10	93	5.0	348.3	51.5	70.1	216.9
159	9/ 8	265	3.4	109.5	72.4	40.1	32.4
161	12/11	504	2.0	110.4	80.5	41.1	30.0

Table 4 (continued)

EC	n_s/n	k	α_{95} (°)	Dec (°E)	Inc (°)	Lat (°N)	Long (°E)
167	11/ 9	151	4.2	340.3	66.8	77.3	280.3
169	28/20	168	2.5	7.9	64.6	83.6	129.1
191	13/13	101	4.1	12.2	69.0	82.0	74.9
170a	13/12	164	3.3	353.1	70.2	84.1	323.6
170b	10/ 9	344	2.7	13.9	66.3	80.8	100.3
176	13/13	305	2.3	105.5	77.1	38.8	37.8
204	12/12	201	3.0	3.4	63.1	84.0	163.0
207a	10/10	719	1.8	357.0	63.0	84.3	209.1
207b	14/12	268	2.6	355.7	55.6	86.3	239.0
208a #	10/10	421	2.3	5.8	66.1	85.8	118.3
208b #	11/ 9	45	7.7	359.9	53.3	73.7	187.2
208c #	14/13	40	6.6	351.5	59.7	78.7	222.2
212	12/12	251	2.7	329.0	69.7	70.6	298.9
213 #	10/ 8	146	4.6	338.2	65.0	68.8	280.6
215a #	11/11	432	2.2	333.7	66.2	72.9	281.8
215b #	10/ 9	30	9.4	335.4	59.0	69.8	255.3
215c #	10/ 9	386	2.6	326.0	68.3	68.6	293.7
215d #	Only NRM-measurements available						
220	8/ 7	462	2.8	4.5	63.1	83.6	156.3
221a	9/ 9	398	2.5	13.3	64.2	80.2	116.8
221b	9/ 9	115	4.8	19.5	69.3	77.5	76.3
223	10/ 8	300	3.2	357.4	67.8	88.2	300.3
224	10	No stable remanence was determined					
6a, b	18	102	3.7	62.4	73.5	54.3	57.5
30, 80a, b	27	59	3.6	349.6	61.0	79.1	231.7
32, 37	17	84	3.9	14.9	66.5	80.3	98.7
41, 43	27	224	1.9	91.6	71.2	38.8	52.8
61, 62	25	98	2.9	56.7	74.7	57.5	55.0
72a, 76	19	241	2.1	93.1	77.3	43.3	44.1
97, 101	18	116	3.2	17.4	75.7	74.2	36.7
99a, b	20	65	3.9	28.7	65.8	71.2	92.5
157a, b	15	90	3.8	57.1	52.2	45.1	97.1
159, 161	19	375	1.6	109.9	80.0	40.7	31.1
169, 170a, b	41	135	1.9	5.6	66.8	86.3	107.2
204, 207a, b, 208c #	47	98	2.6	356.6	63.7	84.6	213.2
212, 215c #	21	298	1.8	327.7	69.1	69.9	269.3
213 #, 215b, c #	28	71	3.3	335.6	63.6	72.9	269.2

of the West Eifel much better and the χ^2-test shows no significant difference (Table 5), although the azimuthal distribution remains non-Fisherian.

Discussion of low-latitude VGPs

Different processes may have resulted in the anomalous low-latitude pole positions: measuring errors, tectonic rotation and tilting, alteration of oxides, anisotropy of magnetization.

Systematic measuring and/or evaluation errors can be excluded. Sampling, measuring and evaluation were done by different workers (Haverkamp, 1980; Jäger, 1982; Reismann, 1985), giving identical results for different sites of the same eruption centre. Special attention was paid to sites showing low-latitude VGPs using different af-demagnetization techniques: static demagnetization as well as different 2- and 3-axes tumblers. Stepwise thermal demagnetization results of selected specimens fully agree with results from af demagnetization.

Tectonic rotation or tilting of sites is improbable but can not be excluded for individual cases. Nevertheless, for the sites in question this was checked in the field at least twice and no evidence for such tectonic effects was found. Moreover, it is unlikely that all sites could have been displaced accidentally in the same manner, as would be implied by the restriction of their VGPs to a well-defined longitude sector. On the other hand, a common movement of all sites with low-latitude VGPs by regional tectonic processes can be excluded, because these sites are distributed throughout the main part of the volcanic field (cf. Fig. 1 and Table 4), only being absent from the SE part of the field.

We have found no correlation between the oxidation state or occurrence of secondary magnetic minerals, nor the magnetic properties, and the low-latitude of VGPs. Oxidation, maghemitization and/or hydrothermal alteration are thus not responsible for the anomalous pole positions. Likewise, there is no correlation of the rock types sampled (scoria, dikes, etc.) with the VGP latitude. On the other

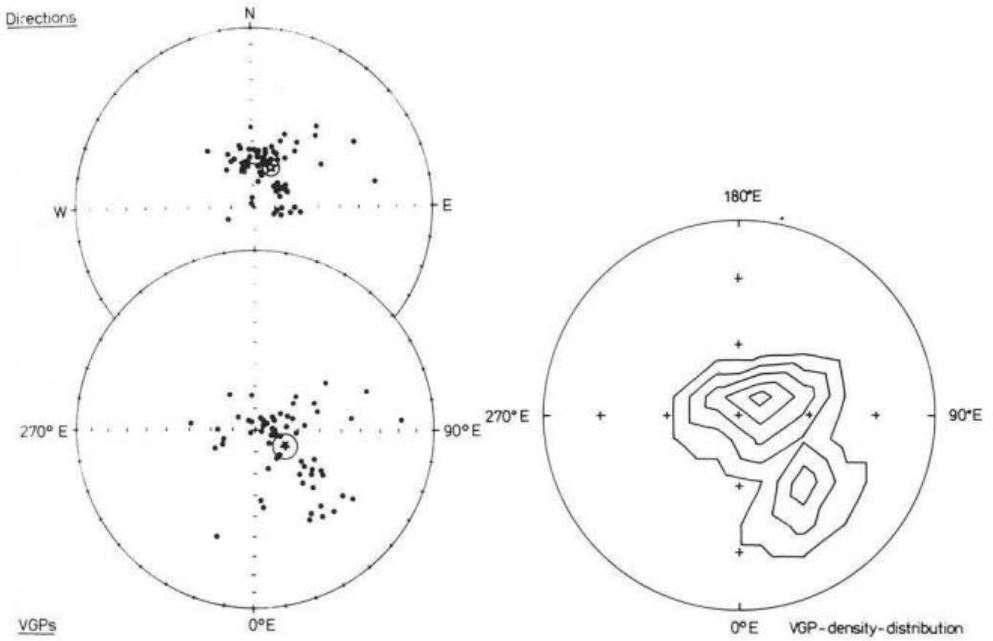

Fig. 5. Site mean directions and VGPs of 64 independent volcanoes. (a) *Points* directions or VGPs, *star* mean direction or VGP, with 95% error limit, respectively; *arrow* dipole field direction. (*b*) VGP density distribution, *lines* represent constant number of VGPs per unit area

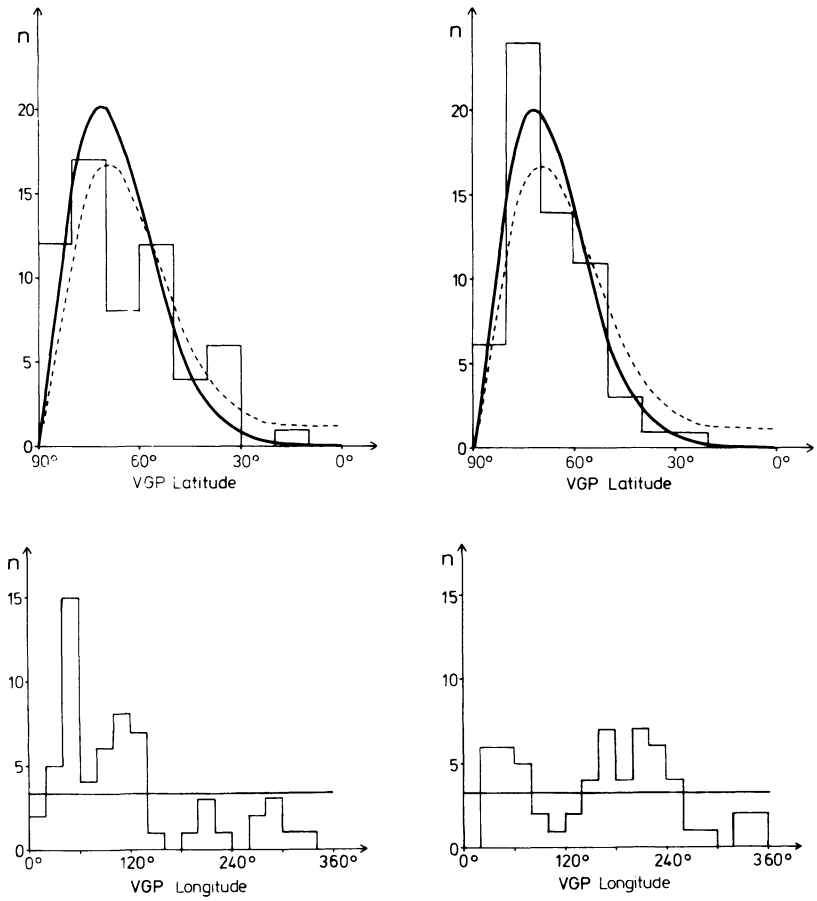

Fig. 6. Theoretical Fisherian distribution (*solid line*) and observed distribution for the West Eifel (*step function*) and the distribution obtained from 2462 Tertiary to Quaternary Icelandic lavas (Kristjansson and McDougall, 1982), relative to the north geographic pole (*left*) and the mean VGP (*right*), respectively. n: number of VGPs per latitude increment or longitude segment (this study)

Table 5. Comparison of VGP distributions around the north geographic pole (NGP) and the mean VGP with a Fisherian distribution by means of the χ^2-test

	Azimuthal distribution		Radial distribution	
	$\chi^2_{obs.}$	$\chi^2_{95\%}$	$\chi^2_{obs.}$	$\chi^2_{95\%}$
Mean VGP	45.63	27.59	4.32	14.07
NGP	74.52	27.59	30.85	14.07

Table 6. Anisotropy of magnetic susceptibility. Eruption centre; number of samples measured; site mean direction of principle anisotropy axes; site mean direction and corresponding VGP

No.	Mean principle anisotropy axis					Paleo-direction		Paleo-pole	
	n	k	α_{95} (°)	Dec (°E)	Inc (°)	Dec (°E)	Inc (°)	Lat (°N)	Long (°E)
20	9	2.7	39.3	7.1	50.2	102.7	73.8	36.4	44.2
6	9	3.1	34.8	20.0	19.2	94.3	70.7	31.1	52.4
28	8	1.2	43.5	324.9	39.0	88.9	71.7	40.4	53.0
38	8	5.9	24.8	49.4	36.6	55.7	75.9	58.1	51.3
8	9	2.7	39.5	138.5	5.5	110.4	80.5	41.1	30.0
40	10	1.7	54.5	221.2	−5.6	105.5	77.1	38.8	37.8
46	10	2.6	40.7	258.4	34.8	58.4	33.8	34.2	109.2
67	9	2.9	36.9	138.5	5.5	110.4	80.5	41.1	30.0

hand, there are no volcanoes of the ONB (olivine nephelinite and basanite) group among the anomalous samples. These are restricted to the SE part of the field and are younger than 0.1 M.a. Any magnetic property determined (magnetization intensity, susceptibility, Königsberger factor, medium destructive field, hysteresis parameters) as well as within-site dispersion parameters k and α_{95} show no relation with VGP latitude.

Anisotropy of magnetic susceptibility (AMS) was measured for samples of selected sites exhibiting anomalous pole positions (Table 6). The low values of the precision parameters k and α_{95} indicate that no preferred anisotropy direction (defined by the principal axes of AMS) exists in any of the sites, and therefore no correlation with the respective paleodirections.

We conclude that the observed low-latitude VGPs are not the result of any extraordinary process having changed the original magnetization, nor of anisotropy of magnetism, nor of tectonic processes. Obviously the paleodirections are reliable and represent real variations of the earth's magnetic field. Finally, a very strong argument for this interpretation is the coincidence of paleodirections from different sites with anomalous pole positions, included in the lower part of Table 4. Many sites are separated by several hundreds of metres and sometimes the rock type differed (scoria, lava flow, dike etc.; cf. Table 1 and Table 4).

The low latitude of many VGPs obtained, together with the restriction of a well-defined longitude sector, rules out the possibility that this could be due to secular variation. More probably, these VGPs represent the earth's magnetic field during excursions or polarity transitions. Kristjansson

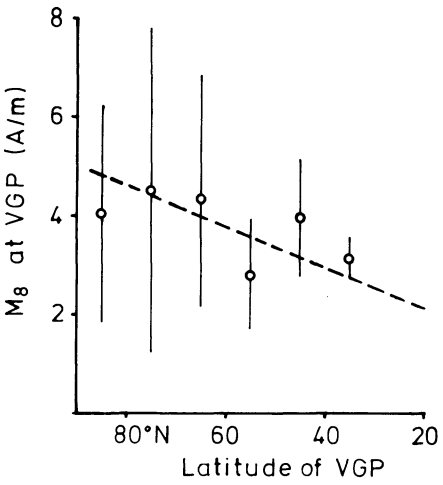

Fig. 7. Arithmetic mean of remanence intensities M_8 (af demagnetized with 8 kA/m) after transformation to virtual geomagnetic pole by 10° increments in VGP latitude. *Dashed line* represents trend observed for Tertiary to Quaternary Icelandic lavas (Kristjansson and McDougall, 1982)

and McDougall (1982) ascribe the low-latitude VGPs of Icelandic lavas to excursions and polarity transitions. This is supported by the positive correlation of remanence intensity M_8 [magnetization intensity after af demagnetization with 8 kA/m and thus more or less representing the thermoremanence TRM, which linearly depends on the field intensity; see, e.g. Day (1977)] with VGP latitude. Such a correlation is to be expected because of the reduction of the field intensity during polarity transitions or excursions as aborted polarity transitions (Jacobs, 1984).

Arithmetic means of remanence intensities M_8 after af demagnetization with 8 kA/m are given in 10°-latitude increments and compared with the line fitting the data from Iceland (Kristjansson and McDougall, 1982) (Fig. 7). The standard deviation is large for the West Eifel data, which is a result of the comparatively small number of data and the heterogeneity of rock magnetic properties. Nevertheless, a similar trend is recognizable. The low-latitude VGPs observed in the West Eifel probably represent the magnetic field during one of the excursions or events in the Brunhes epoch. According to the age range of the corresponding volcanoes of 0.1–0.4 M.a., four events have to be considered: Blake, Biwa I and II and the Emperor event (Jacobs, 1984). The duration of these events was less than about 0.03 M.a., but the restriction of the VGPs to a small longitude sector seems to imply a much smaller period of volcanic activity. Consequently, if a magnetic excursion is the reason for the anomalous VGPs, this would confine the age of a considerable part of all West Eifel volcanoes to a very small period compared to the total period of volcanic activity. All samples are from volcanoes within the main field, i.e. the F-suite magmas (Schmincke, 1982; Mertes and Schmincke, 1985), none from the SE subfield (i.e. ONB-suite magmas). We thus conclude that eruption of F-type magmas in the main part of the West Eifel field occurred in at least two different phases, one of which is correlated with a period of anomalous low latitudes of magnetic poles. This interpretation raises the question of eruption frequency during the evolution of the entire volcanic field. Recent high-precision dating of basanite volcanoes in the East Eifel has shown that most erupted during a relatively short time span, ca. 0.2–0.25 M.a. (Bogaard et al., 1986). It would be interesting to study the radiometric ages of the volcanoes with low VGP in detail in order to define the evolution of volcanic periodicity more precisely.

Acknowledgements. This investigation was financially supported by the Deutsche Forschungsgemeinschaft (funds UN 29/24, 29/29-2, 29/29-3). Prof. Dr. H.U. Schmincke would like to thank the Ministerium für Wissenschaft und Forschung, NRW, for general financial support of the Eifel project. It is appreciated that Dr. N. Nun made most of the SEM studies.

References

Ade-Hall, J.M., Khan, M.A., Dagley, P., Wilson, R.L.: A detailed opaque petrological and magnetic investigation of a single Tertiary lava from Skye, Scotland. Part I and II. Geophys. J. R. Astron. Soc. **16**, 374–399, 1968

Böhnel, H., Kohnen, H., Negendank, J., Schmincke, H.-U.: Paleomagnetism of Quaternary volcanics of the East-Eifel, Germany. J. Geophys. **51**, 29–37, 1982

Bogaard, P. van den, Hall, C.M., York, D., Schmincke, H.-U.: High precision single grain 40 Ar/39 Ar laser ages from Pleistocene tephra deposits, East Eifel volcanic field, FRG. Eos **67**(44), 1248, 1986

Büchel, G., Lorenz, V.: Zum Alter des Maarvulkanismus der Westeifel. Neues Jb. Geol. Paläont. Abh. **163**, 1–22, 1982

Büchel, G., Mertes, H.: Die Eruptionszentren des Westeifeler Vulkanfeldes. Z. Dt. geol. Ges. **133**, 409–429, 1982

Collinson, D.W.: Methods in rock magnetism and palaeomagnetism. London-New York: Chapman & Hall 1983

Day, R.: TRM and its variation with grain size. J. Geomagn. Geoelectr. **29**, 233–265, 1977

Day, R., Fuller, M., Schmidt, V.A.: Hysteresis properties of titanomagnetites. Grain-size and compositional dependence. Phys. Earth Planet. Inter. **13**, 260–267, 1977

Duda, A., Schmincke, H.-U.: Polybaric evolution of alkali basalts from the West Eifel: evidence from green-core clinopyroxenes. Contr. Mineral. Petrol. **91**, 340–353, 1985

Dunlop, D.J.: The rock magnetism of fine particles. Phys. Earth Planet. Inter. **26**, 1–26, 1981

Fisher, R.A.: Dispersion on a sphere. Proc. R. Soc. London **A-127**, 295–305, 1953

Haverkamp, U.: Paläomagnetische Untersuchungen an quartären Vulkaniten der Westeifel. Diploma thesis, Inst. Geophys. Münster, 1980

Hoffman, K.A., Day, R.: Separation of multi-component NRM: a general method. Earth Planet. Sci. Lett. **40**, 433–438, 1978

Illies, H.J., Prohdehl, C., Schmincke, H.-U.: The Quaternary uplift of the Rhenish Shield in Germany. Tectonophysics **61**, 197–225, 1979

Jacobs, J.A.: Reversals of the earth's magnetic field. Bristol: Adam Hilger Ltd. 1984

Jäger, G.: Paläomagnetische Untersuchungen im quartären Vulkanfeld der Westeifel. Diploma thesis, Inst. Geophys. Münster, 1982

Kirshvink, J.L.: The least-squares line and plane and the analysis of palaeomagnetic data. Geophys. J.R. Astron. Soc. **62**, 699–718, 1980

Kohnen, H., Westkämper, H.: Palaeosecular variation studies of the Brunhes epoch in the volcanic province of the East-Eifel, Germany. J. Geophys. **44**, 545–555, 1978

Kristjansson, J., McDougall, I.: Some aspects of the late Tertiary geomagnetic field in Iceland. Geophys. J.R. Astron. Soc. **68**, 273–294, 1982

Likhite, S.D., Radhakrishnamurty, C., Sasharabudhe, P.W.: Alternating current electromagnet type hysteresis loop tracer for minerals and rocks. Rev. Sci. Instr. **36**, 1558–1560, 1963

Lippolt, H.J., Fuhrmann, U.: Isotopische Altersbestimmungen an tertiären und quartären Vulkaniten des Rheinischen Schildes.

DFG Protokoll 5. Kolloquium Schwerpunkt Vertikalbewegungen, Neustadt 1980, 171–176, 1981
Mertes, H.: Aufbau und Genese des Westeifeler Vulkanfeldes. Bochumer geol. and geotechn. Arb. **9**, Bochum, 1983
Mertes, H., Schmincke, H.-U.: Age distribution of volcanoes in the West Eifel. N. Jb. Geol. Paläont. Abh. **166**, 260–293, 1983
Mertes, H., Schmincke, H.U.: Mafic potassic lavas of the Quaternary West Eifel volcanic field. I. Major and trace elements. Contrib. Mineral. Petrol. **89**, 330–345, 1985
Molyneaux, L.: A complete result magnetometer for measuring the remanent magnetization of rocks. Geophys. J. R. Astron. Soc. **24**, 429–433, 1971
Reismann, N.: Abschließende paläomagnetische Untersuchungen der Verteilung der virtuellen geomagnetischen Pole für das quartäre Vulkanfeld der Westeifel. Diploma thesis, Inst. Geophys. Münster, 1985
Sachtleben, T., Seck, H.A.: Chemical control on Al-solubility in orthopyroxene and its implications on pyroxene geothermometry. Contrib. Mineral. Petrol. **78**, 157–165, 1981
Schmincke, H.-U.: Vulkane und ihre Wurzeln. Rhein. Westf. Akadem. Wiss., Westd. Verl. Opladen, Vortrag N 315, 35–78, 1982
Schmincke, H.-U., Lorenz, V., Seck, H.A.: The Quaternary Eifel volcanic fields. In: Mode and mechanics of the uplift of the Rhenisch Shield: a case history, K. Fuchs et al., eds.: pp. 139–151. Heidelberg – New York – Tokyo: Springer Verlag 1983
Stosch, H.G., Seck, H.A.: Geochemistry and mineralogy of two spinel peridotite suites from Dreiser Weiher, West Germany. Geochim. Cosmochim. Acta **44**, 457–470, 1980
Symons, D.T.A., Stupavsky, M.: A rational palaeomagnetic stability index. J. Geophys. Res. **79**, 1718–1720, 1974
Wilson, R., Haggerty, S.E.: Reversals of the earth's magnetic field. Endeavour **25**, 103–109, 1966
Zijderveld, J.D.A.: A.c. demagnetization of rocks: analysis of results. In: Methods in palaeomagnetism, D.W. Collinson, K.M. Creer and S.K. Runcorn, eds. Amsterdam: Elsevier 1967

Received March 17, 1987; revised version June 25, 1987
Accepted June 26, 1987